Power System Technology
ISSN:1000-3673

Received: 16-01-2024 *Revised: 12-02-2024* *Accepted: 07-03-2024*

Integrated Energy Storage System Based Efficient Wireless Charging for Ev Topology

Karthick S[1], Selvan P[2] Akilan Vishnu G[3], Hariprasanth C[4],
[1]Associate Professor, Electronics and Communication Engineering, Erode Sengunthar Engineering College, Perundurai, India
[2] Professor Electrical and Electronics Engineering, Erode Sengunthar Engineering College, Perundurai, India
[3,4] Electrical and Electronics Engineering, Erode Sengunthar Engineering College, Perundurai, India
researchkarthick@gmail.com

Abstract - Power transfer without the need of wires or other electrical conductors of any kind. In order to minimise transmission, allocation, and other kinds of losses have put out a theory that is covered in this discussion on the use of microwaves to convey electricity. This method is referred as microwave power transmission (MPT). Along with the evolution of wireless power transmission systems and the associated developments and also described and connected a number of elements of the power transmission methods that are now on the market Also covered the fundamentals of wireless power transmission (WPT), its advantages and disadvantages, and its uses. Due to arbitrary charging control brought on by their increasing popularity, a sizable number of electric cars (EVs) will pose a burden on the grid in the future. In order to make EVs compatible with the grid, controlling the vehicle's charging and discharging conditions is crucial. Thus, this study proposes a bidirectional PV battery-assisted EV parking lot design with vehicle-to-grid service using a multiport DC-DC solid state transformer structure, taking into account the possibility that EVs would be seen as energy storage devices. In this paper, a system Grid to vehicle and vehicle to grid power transfer, EVs are charged by wireless power transfer method in the parking slot is presented.

Keywords - PV, EV, Wireless Power Transmission (WPT), Wireless Charging for EV, Converters

1. Introduction

The demand of EVs has spurred the growth of numerous charging techniques, with wireless chargers appearing as a potential substitute for traditional cable charging. The creation of an electric car wireless charging station is going to be the main focus of this work. The wireless charging system for the EV is composed of the charging station and receiving unit. The EV's battery is recharged by means of a current of electricity that is experienced by the receiver device due to the magnetic field produced by the charging surface. A multitude of considerations go into the layout of the wireless charging structure, including selecting the appropriate parts, optimizing the system's efficiency, and meeting safety regulations [1-3].

One important new development in the area of power circuits is the rapid charging of EVS via WPT. The size of the primary storage battery may be lowered, greatly lowering the price,

Power System Technology
ISSN:1000-3673
Received: 16-01-2024 Revised: 12-02-2024 Accepted: 07-03-2024

weight, and usage of elements made of rare earths, by lowering the need for all of the power needed for a trip within the vehicle. A vehicle-mounted coil passes across primary pads, which are embedded coils in the road, in a conventional dynamic electrical charging system that operates in a sequential manner [4-7]. Power may be supplied to the EV using a magnetic connection between its coils. A number of isolated coils have been shown to be more realistically viable than just one unbroken the right path, as is so with other systems using WPT. A main pad that is provided by the grid wirelessly transmits power to a pad that is positioned beneath an EV via magnetic coupling in an ordinary WPT charging arrangement. At an ordinary inductive power transfer (IPT) frequency of operation of 85 kHz, the ground pad set has to be carefully energised in parts less than the total length of the vehicles going over it. The implementation of the dynamic charging in real-world systems faces a number of noteworthy obstacles [8,9]. The extremely powerful pulses produced by the discontinuous power transmission need to be handled by the EV's electrical system. The EV battery is overheated and deteriorated when a strong current burst is directly fed into it [10]. The entering burst of energy needs to be kept another way because the ultimate goal of rapid charging is to enable smaller batteries with corresponding reduced maximum charge ratings for power. Super capacitors (SCs) have formed the basis of immediate, high-density storage of energy that has been suggested for dynamic charging purposes. The ease and durability of connecting the SC directly to the EV dc bus are advantages, however the restricted voltage swing causes a poor utilisation of the SC’s battery capacity [11, 12]. Although it comes with more expense, complexity, and components, using a specialised dc-dc converter to link the SC to the EV dc bus gives good utilisation and management. Using an energy reserve on a charging the system’s main side lowers the grid’s highest demand and enhances the power factor. To link an EV dc bus, a fuel cell made of hydrogen, and other powerful power source like a flywheel or SC, multiport dc-dc converters were created. The power needed by the EV’s propulsion systems and the speed at which it charges are the main determinants of the amount of energy storage needed for a dynamic charging device. While the EV battery can manage power variations over a long period of time, the substantial amount of extra energy storage is best suited for handling short-duration power variations, which are common in pulsed charging. Flywheels are one type of energy storage device that has been created for light rail uses, however at this stage of growth, it is not suited for automobile uses [13-15]. The well recognised answer to the issue of handling extremely high energy pulses experienced during the dynamic charging of EVs is a bank of SCs acting as an energy buffer. The effectiveness, price, size, and dependability of the entire charging mechanism are jeopardised as the SC voltage is incompatible with the EV’s propulsion system and must thus be incorporated into the EV utilising a separate converter stage. It is now possible to integrate storage of energy in a SC with an IPT system that utilises a single converter thanks to a newly designed architecture. But because the SC current must pass via the IPT pad, there are more losses. A different approach is to divide the H-bridge’s sides into half bridge so that their respective de bus voltages may be independently controlled, enabling power factor adjustment [16-19].

Energy may be freely transferred between the input, output, and storage areas of the suggested converter. The de current that passes via the IPT pad and compensating system is eliminated in this configuration by connecting the SC and converter in this way. The voltage

Power System Technology
ISSN:1000-3673

Received: 16-01-2024 *Revised: 12-02-2024* *Accepted: 07-03-2024*

waveform supplied to the IPT pad and compensating networks in the setup suggested in this paper is without dc offset and is similar to the symmetric three-level waveform seen in a typical IPT converter, which is an additional advantage over earlier methods[20,21]. For an electrical switching conversion, the link of a SC to the common mode voltage of a dc-ac converter is shown, and for a three-phase converter, the connecting of a dc source to its common mode value is shown. The connecting of a dc port to an H-bridge's standard mode output in a resonant converter for EV charging purposes is shown in this paper [22-25].

In this paper, a system Grid to vehicle and vehicle to grid power transfer, electric vehicles are charged by wireless power transfer method in the parking slot is proposed. Consequently in this study, a multiport DC-DC solid state transformer design with vehicle-to-grid service is proposed for bidirectional PV battery-assisted electric car parking lots, taking into account the possibility that EVs would be seen as energy storage devices.

2. Materials and Methods

A Proposed System

Using inductive coupling for WPT is one of the most efficient ways to move electricity between locations without a traditional wire network. In locations where cable systems are difficult or impossible to access, wireless power transmission works well. Based on if the energy is being transported across a short, mid, or long distance, it can be done so by electromagnetic transfer, resonance induction, or inductive coupling. The purpose of this research is to use wireless power transfer for charging a low power device through the use of an inductive coupling charging device. In order to do this, a resonant coiled is charged with AC power before electricity is subsequently sent to the resistive load. The effort aims to quickly and efficiently charge a low-power device without using connections.

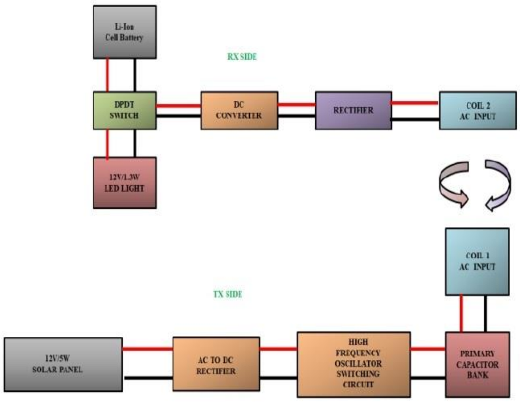

Figure 1 (Proposed System)

The wireless charger in this work primarily on the inductive coupling technique. The schematic makes it evident that the wireless charger network needed both a WPT and a wireless power receiver component in order to operate as a whole. This WPT section's

Received: 16-01-2024 *Revised: 12-02-2024* *Accepted: 07-03-2024*

transmitter coil transforms DC electricity from an oscillator into a high-frequency AC power signal. In order to transfer energy, a high-frequency AC connected to the WPT coil would induce a magnetic field that is alternating inside the coil. The rectifier in the wireless energy receiver segment transforms the AC voltage that the receiving coils in the area acquire as an induced alternating voltage into a DC voltage. Ultimately, a voltage controller component would supply the rectified DC voltage to the load. In other words, the primary purpose of the wireless power receiver part is to use inductive coupling for charging a low power battery. The two primary elements of the work are the wireless power receiver and transmitter portions. A transmitter coil, an oscillator, and a DC power supply make up the transmitter portion of the wireless charger network. A DC power supply produces a steady DC voltage, which serves as the oscillator circuit's input. This DC voltage is transformed by this oscillator into high frequency AC power, which is then sent into the transmission coil. The transmitter coil energizes and creates a magnetic field that is alternating inside the coil as a result of this high frequency AC current. The source of electricity is made up of a circuit with a rectifier to turn the AC voltage into a DC signal and a step-down transformer that is used to reduce the supply voltage to a desirable level.

B. Basic Solar Cell Modeling

A resistance Rs coupled in series with a source of current made up of a single diode and a shunt resistance architecture RS is used to produce a single solar cell. Solar energy is directly converted into electric energy by a solar cell via the photoelectric effect. As a result, when light strikes an electrical component, its characteristics such as resistance, voltage, and current change. Electric current is produced as a result, independent of any external voltage source. An external load is connected to determine power usage.

Before building a solar cell, the following equations must be solved:
Thermal voltage equation

$$v_T = k_B T_{OPT}/q \quad (1)$$

Diode current equation

$$I_D = N_P - I_S[e^{\left(\frac{V}{Ns}\right)+\frac{(\frac{IRs}{Ns})}{NV_T C-1}}] \quad (2)$$

Load current equation

$$I_L = I_{ph}N_p - I_D - I_{SH} \quad (3)$$

Photocurrent equation

$$I_{ph} = [k_i(T_{OPT} - T_{REF})I_{SC}]I_{RR} \quad (4)$$

Shunt current equation

Power System Technology
ISSN:1000-3673

Received: 16-01-2024 Revised: 12-02-2024 Accepted: 07-03-2024

$$I_{SH} = (I_{RS} + V)/R_{SH} \qquad (5)$$

Reverse Saturation current

$$I_S = \left[I_{RS} \left(\frac{T_{OPT}}{T_{REF}} \right)^3 * \frac{q^2 Eg}{N k_B} * e^{\left(\frac{1}{T_{OPT}} - \frac{1}{T_{REF}} \right)} \right] \qquad (6)$$

Reverse current equation

$$I_{RS} = \left[\frac{I_{SC}}{e^{(q v_{OC} k \, CT_{iOPT})}} - 1 \right] \qquad (7)$$

Output power

P = VI (8)

Where V_T is the Thermal Voltage and V_J is the Junction Voltage, V_{OC} is the Voltage on Open Circuit, Iph is the Irradiation and junction temperature photocurrent function, Is is the diode's reverse saturation current and I_{ph} is the amps of short circuit current. T_{REF} stands for the cell's reference operating temperature and T_{OPT} is the Cell Operational Temperature (°C), R_{SH} is the cell's shunt resistance, R_s is the cell's series resistance.

The behaviour of a solar cell is ascertained by the creation of an electrical de equivalent model. A current source connected in parallel to a diode can be used to simulate a perfect solar cell. However, in real life, no solar cell is perfect, thus the model is expanded to include an adequate shunt resistance element and an analogous tiny series resistance. In an ideal world, it would be built with constant values that match the previously listed STC (Standard Test Conditions).

The following diagram represents a solar cell's DC equivalent network:

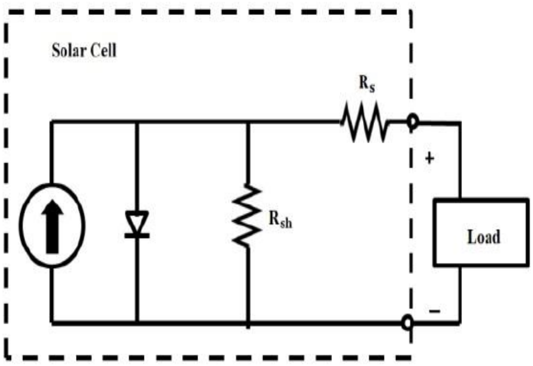

Figure 2 (DC Equivalent Model of Solar Cell)

Received: 16-01-2024 Revised: 12-02-2024 Accepted: 07-03-2024

It is clear from the equivalent diagram that the voltage generated by the solar cell corresponds to the current generated by the current source $I_p\ N_p$, less the current that passes through the diode I_D and the shunt resistor I_{SH}, as stated:

$$I_L = I_{ph}N_{p-}I_D - I_{SH} \qquad (9)$$

The voltage across these components controls the current flowing through that

$$V_J = V + IR_S \qquad (10)$$

The following Shockley's formula governs diode current:

$$I_d = N_P I_S[e^{\left(\frac{V}{Ns}\right)+(\frac{IR_S}{N_S})NV_T{}^{C-1}} \qquad (11)$$

The current flowing across the shunt resistor is determined by Ohm's Law to be

$$I_{SH} = \frac{V_J}{R_{SH}} \qquad (12)$$

$$I_{SH} = (V + IR_S)/R_{SH} \qquad (13)$$

Using these formulas in place of the other equation to calculate the load current

$$I_L = I_{ph}N_p - N_p I_S\left[e^{\left(\frac{V}{N_S}\right)+(IR_S)}NV_{T^{C-1}}\right] - (IR_s + V)/R_{SH} \qquad (14)$$

Thus, the operating current (I_L) at a given operating voltage V may be found by solving the equation.

The maximum current that can be extracted from a solar cell at zero voltage, which is produced by the creation and accumulation of carriers created by light, is known as the short-circuit current (S_{CC}). The greatest voltage that a solar cell can produce in relation to the amount of forward bias that the solar cell experiences as a result of zero current is known as the open- circuit voltage, or Voc

Generally speaking, a solar cell may give a maximum power of P_{MAX}=$I_{MAX}V_{MAX}$ created at its output, but not always at STC. On the other hand, I_{SC} and V_{OC}, or the result of OC voltage and SC current, correspond to the optimum maximum power. As a result, the Fill Factor (FF), is computed to describe the experiment output along with the I_{SC} and V_{OC}

$$FF = P_{MAX}/I_{SC}V_{OC} \qquad (15)$$

In terms of graphics, FF represents how squarely the solar cell fits into the Current Voltage

Power System Technology
ISSN:1000-3673
Received: 16-01-2024 *Revised: 12-02-2024* *Accepted: 07-03-2024*

IV curve. Applying the Power Voltage PV curve, the conversion efficiency (η) of solar cells is determined as the ratio of the incident power (P_{IN}) to the produced maximum power (P_{MAX}).

$$\eta = VOC_{ISC}{}^{FF}/_{P_{IN}} \qquad (16)$$

Characteristics of the Maximum Power Point where PV and IV overlap Features are shown in the diagram below:

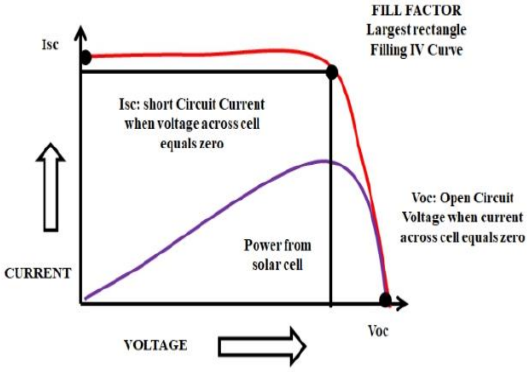

Figure 3 (IV Characteristic Curve of Solar Cell)

B. AC to DC rectifier

An electrical component known as a rectifier converts AC, which often switches directions, into DC, which only moves in one direction. Inverters do the opposite function, converting DC to AC. In earlier times, synchronous electrical switches and motor-generator combinations were additionally used. Placed to the outermost layer of a galena (lead sulphide) crystal, a "cat's whisker" of small wire used as a point-contact converter or "crystal sensor" in earliest radio receivers referred to as "crystal radios." Rectifiers are helpful in many different applications, but they are commonly used in DC power supplies and high-voltage direct current electricity transmission networks. Other uses for rectified current than generating direct current from a power source exist. As has been indicated, rectifiers may be used as detectors of radio signals. In gas heating structures, flame rectifying is utilised to detect the existence of a flame.

To provide a uniform constant voltage, the output voltage may need further smoothing, depending on the kind of AC supply and how the rectifier circuit is configured. Rectifiers are used in many different applications, such power supply for computers, televisions, and radios, which need a stable, continuous DC voltage, which a battery would provide. The rectifier's output can be smoothed in certain situations by an electronic filter, which can be a capacitor, choke, or a mixture of resistors, chokes, and capacitors. A voltage regulator may then be used to generate a constant voltage.

Power System Technology
ISSN:1000-3673
Received: 16-01-2024 Revised: 12-02-2024 Accepted: 07-03-2024

C. Capacitor Bank

A capacitor bank is a type of battery pack consisting of several capacitors connected in series or series. This method enhances energy transfer efficiency in an AC power supply by mitigating phase shift and power factor lag.

D. Principle of WPT

Using inductive coupling for WPT constitutes one of the most efficient ways to move electricity between locations without a traditional wire system. In locations where cable systems are impractical or impossible to access, wireless power transmission works well. Based on if the energy is being transported across a short, mid, or long distance, it can be done so by electromagnetic wave transmission, resonant induction, or inductive coupling. The purpose of this work is to use wireless power transfer for charging a low power device through the use of an inductive coupling charging circuit. In order to do this, a resonant coil is charged with AC power before electricity is subsequently sent to the resistive load.

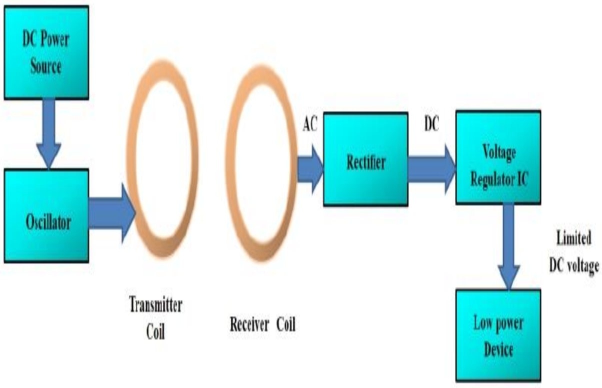

Figure 4 (Block Diagram of WPT Circuit using Inductive Coupling)

The wireless charger in this work primarily on the inductive coupling technique. It is attempting to wirelessly transfer electricity to charge low power gadgets, such as wireless mice, cameras, and cell phones, using the concept of inductive coupling. The schematic makes it evident that the wireless charger circuit needed both a WPT and a wireless power receiver component in order to operate as a whole. This WPT section's transmitter coil transforms DC electricity from an oscillator into a high-frequency AC power output. A rectifier in the wireless power receiver part transforms the AC voltage which the receiver coils in the section acquire as an induced alternating voltage into a DC voltage. Ultimately, a voltage controller component would supply the rectified DC voltage to the load. In other words, the primary purpose of the wireless power receiver part is to use inductive coupling for charging a low power battery.

Power System Technology
ISSN:1000-3673
Received: 16-01-2024 Revised: 12-02-2024 Accepted: 07-03-2024

E. Lithium-Ion Batteries

Many batteries are arranged in both parallel and serial configurations within the battery pack. The battery cells' performance varies when these batteries are used. The inconsistent battery settings are the root reason for efficiency irregularities. It significantly affects the battery pack's lifetime and efficiency. For example, a 20% mismatch in specifications will result in a 40% reduction in lifespan for a cylindrical LiFePO4 battery. When compared to a single battery, it has a much shorter lifespan. To enhance the performance of battery, it is crucial to optimise the battery settings consistently. The study of cell-to-cell differences in resistance, OCV, and SOC parameters that are intimately related to cell sorting has received a lot of interest lately. Sorting batteries entails applying certain techniques to group collectively batteries with comparable efficiency in order to increase battery consistency and lessen the adverse effects of initial distinctions between batteries, ultimately enhancing the batteries' usability and extending their service life. The many techniques for sorting lithium-ion batteries are covered in the next section.

F. State of charge estimation

Every battery cell's voltage and capacity must precisely match the voltage level required by EVs because of electrode potential and material restrictions. As a result, series and parallel connections between thousands of battery cells are required. Although inconsistent battery pack settings and erratic operating circumstances might result in notable variations in battery capacity. Additionally, the precision of the SOC data is crucial for a trustworthy estimate of the remaining EV driving range. A few SOC methods for estimation are introduced in this part.

A low frequency cell difference model (CDM) is used to study the cell voltage differences (CVDs) between the cell and the "mean cell". Variations in SOC and internal resistance are taken into account in this framework. The OCV difference may be estimated using the framework. This approach makes it possible to precisely estimate the SOC discrepancies of lithium-ion batteries while they are being used in EVs using current measuring methods.

The relationship between SOC and OCV is calculated using the aforementioned approach to get the result. All other factors are disregarded. It is necessary to assess the conflicting circumstances in various SOC rates. By applying a developing model-based SOC estimate strategy, a parametric simulation approach is suggested. To rectify the SOC estimation, a three- dimensional reaction surface OC voltage model is suggested, based on the examination of the mapping connection between battery characteristics and SOC. The power source model's schematic layout is displayed in Figure 5. The model is too basic to provide an accurate description of the analogous circuit design.

Power System Technology
ISSN:1000-3673
Received: 16-01-2024 *Revised: 12-02-2024* *Accepted: 07-03-2024*

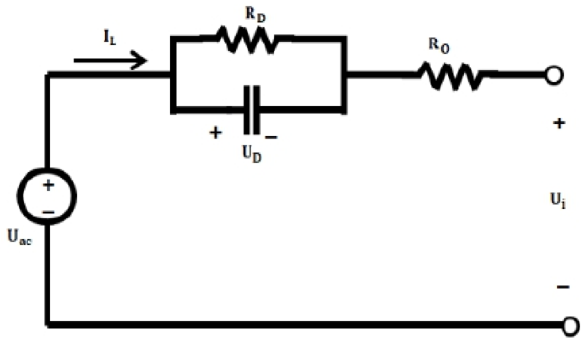

Figure 5 (Lumped battery circuit model)

The estimation of SOC for selected and unselected cells is done by the use of micro and macro time scale approaches, accordingly. According to the findings, for both the battery pack and the unknown diving cycle, the maximum predicted errors of the voltage of the battery and SOC are less than 30 mV and 1%, correspondingly. This approach carried out a more thorough investigation of the effects of the battery's characteristics on SOC in a micro and macro time scale than the M+D model technique did. There is increased accuracy in the battery parameter model. However to improve the calibration performance of this approach, the OCV analytical formulas ought to be rewritten. Currently, this approach is not suitable for batteries that have been deeply depleted.

3. Results and Discussion

To validate the model's correctness and show that the suggested topology is feasible, a demonstration prototype with a nominal power output has been built using the specifications given in Table 1. Though the general idea of operation is the same, the EV system would be able to store far greater energy pulses since it would be equipped with a far greater capacitance compared to the prototype.

Table 1 (Parameters & Rating table)

Parameters	Ratings
Battery	
Battery SOC	80%
Battery Current	30 amps
Battery Voltage	130 V
PV Panel	
Peak power	10 KW
Capacity	5 W
Number of panels	20

Power System Technology
ISSN:1000-3673
Received: 16-01-2024 *Revised: 12-02-2024* *Accepted: 07-03-2024*

Case 1 : At Constant Temperature and Irradiation

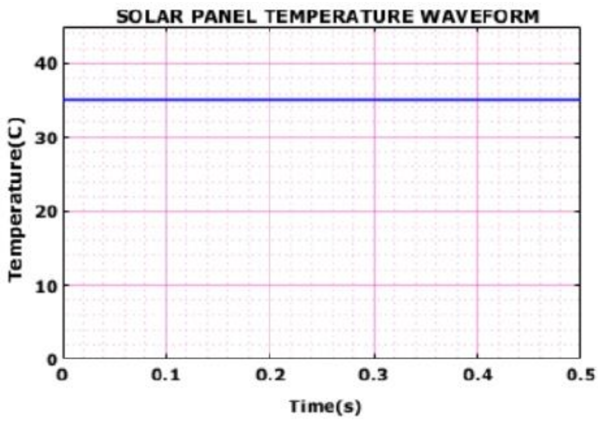

(a)

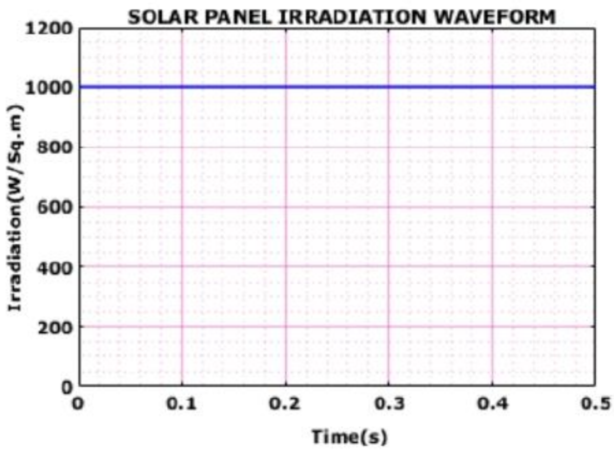

(b)

Figure 6 (Solar Parameter Waveforms (a) Temperature and (b) Irradiation)

Figure 6 shows the characteristics of the solar PV system in relation to radiation and temperature. It is noticed that the typical temperature is 35°C once the sun rises. In a similar manner, the panel radiation is 1000W/sq m, which supplies sufficient electricity to the converter input.

Power System Technology
ISSN:1000-3673

Received: 16-01-2024 *Revised: 12-02-2024* *Accepted: 07-03-2024*

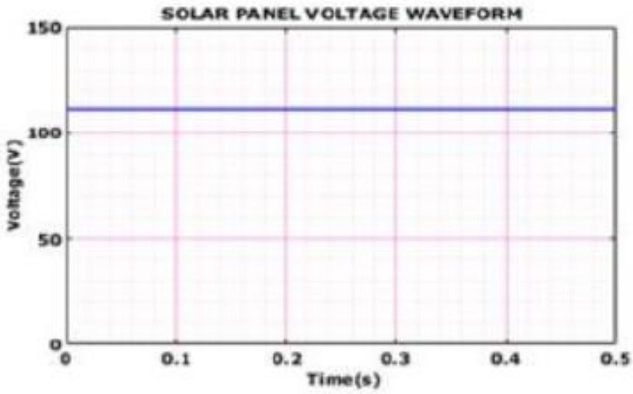

(a)

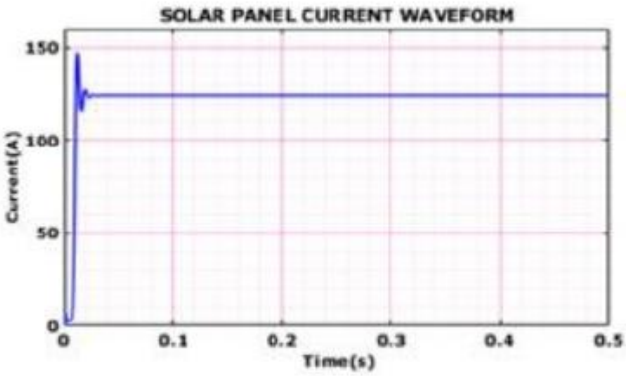

(b)

Figure 7 (Solar Parameter Waveforms (a) Voltage (b) Current)

The electrical voltage and current wave from the solar panel to the converter is shown in Figure 7. A rise in the PV variable leads the voltage to climb to 120V and remains there and steady current level of 125A is reached.

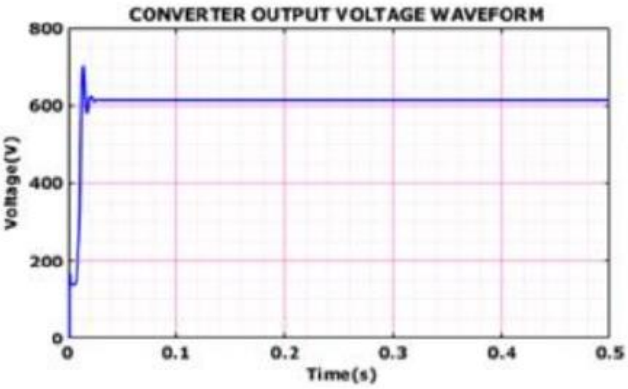

(a)

Power System Technology
ISSN:1000-3673
Received: 16-01-2024 *Revised: 12-02-2024* *Accepted: 07-03-2024*

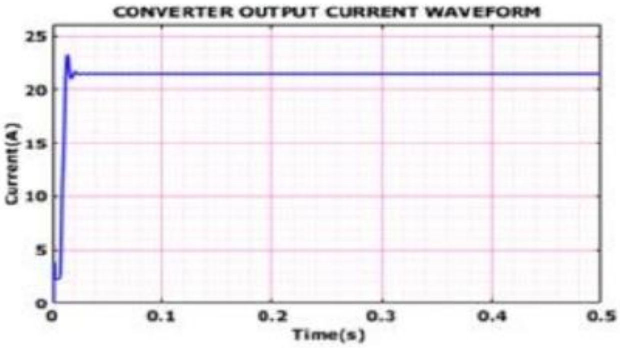

(b)

Figure 8 (Converter output (a) Voltage (b) Current)

Figure 8 displays the converter's correct output current. The current seems to fluctuate at first, but after 0.1 s it stabilises and remains at a constant 22A and maintains a voltage at 610V.
Case 2: Under Varying Condition

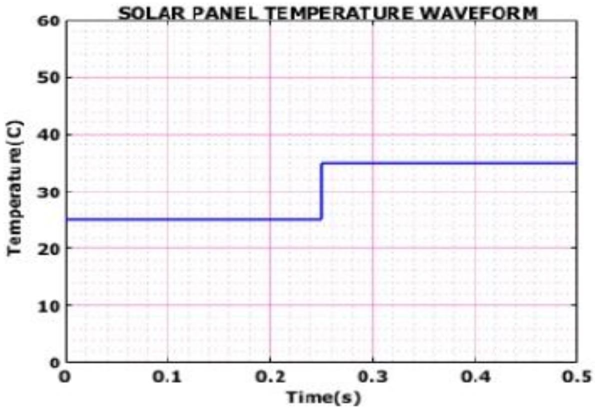

(a)

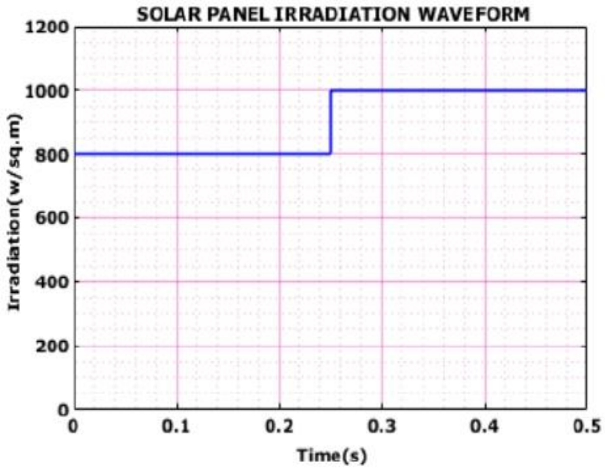

(b)

Figure 9 (Solar Parameter Waveforms (a) Temperature and (b) Irradiation)

Power System Technology
ISSN:1000-3673
Received: 16-01-2024 *Revised: 12-02-2024* *Accepted: 07-03-2024*

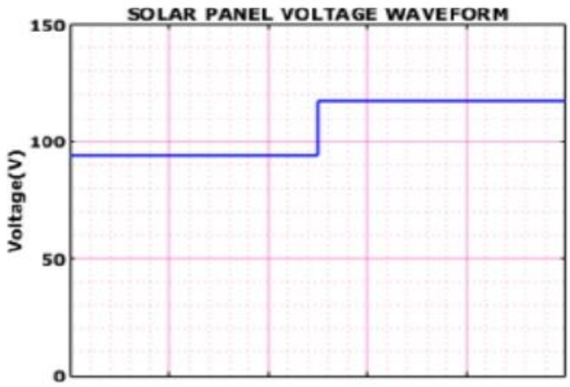

(a)

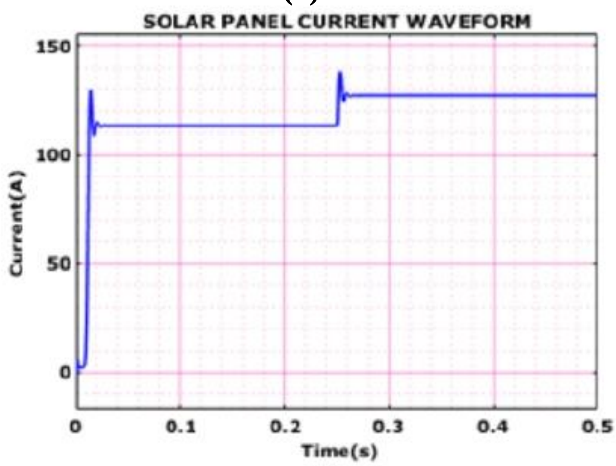

(b)

Figure 10 (Solar Parameter Waveforms (a) Voltage (b) Current)

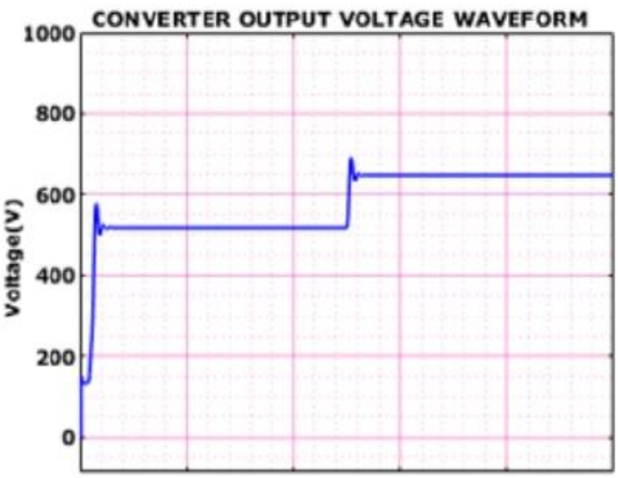

(a)

Power System Technology
ISSN:1000-3673
Received: 16-01-2024 *Revised: 12-02-2024* *Accepted: 07-03-2024*

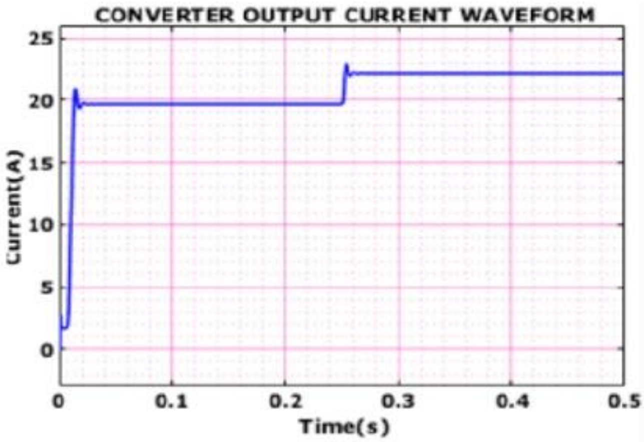

(b)

Figure 11 (Converter output (a) Voltage (b) Current)

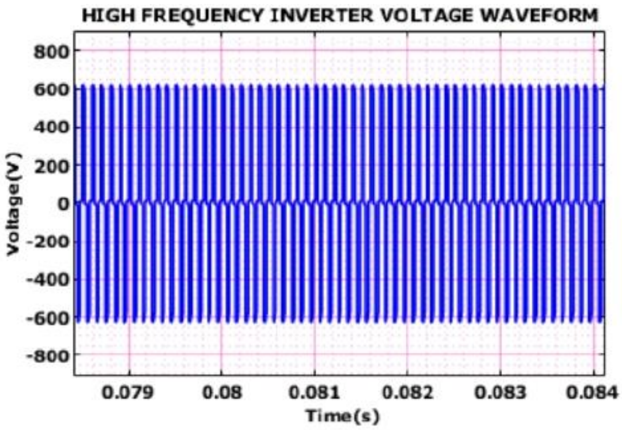

Figure 12 (High frequency inverter voltage)

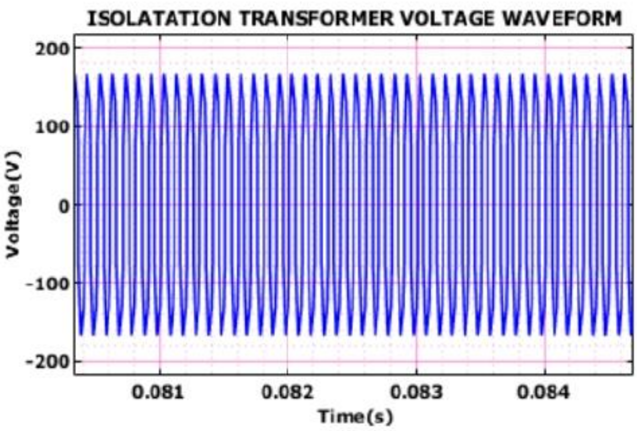

Figure 13 (Isolation transformer voltage)

Power System Technology
ISSN:1000-3673
Received: 16-01-2024 Revised: 12-02-2024 Accepted: 07-03-2024

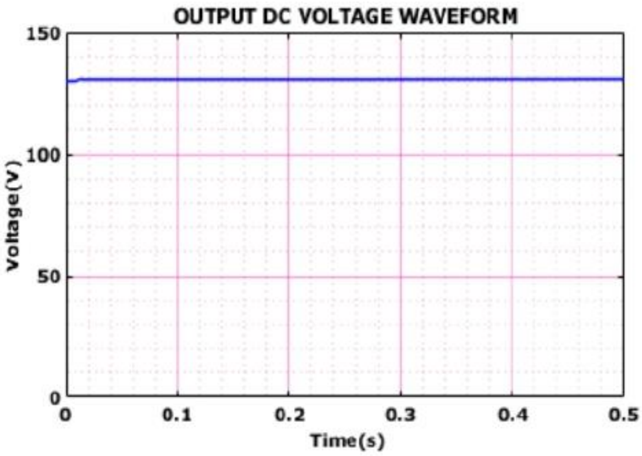

Figure 14 (DC output Voltage)

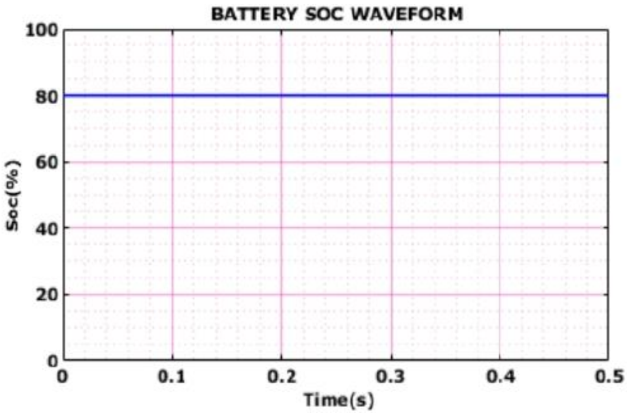

(a)

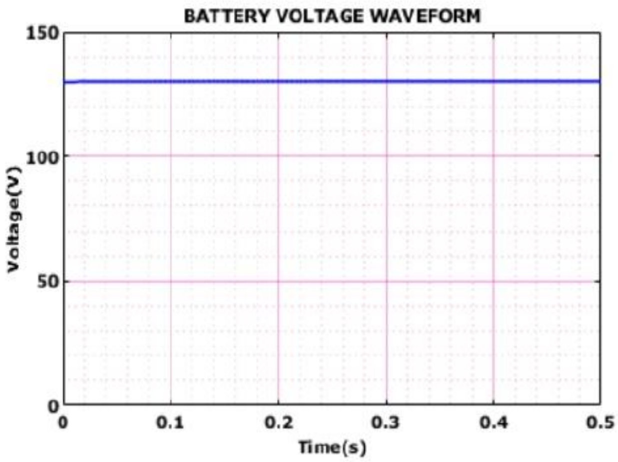

(b)

Power System Technology
ISSN:1000-3673
Received: 16-01-2024 *Revised: 12-02-2024* *Accepted: 07-03-2024*

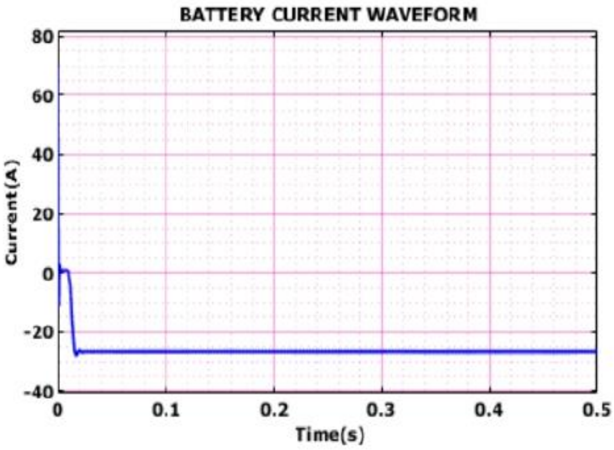

(c)

Figure 15 (Battery output (a) SOC (b) Voltage (c) Current)

As shown in figure 15, the battery cell was running at 30A continuous current and 130V battery voltage and the battery's SOC reached 80%.

4. Conclusion

This paper discusses the ideas behind WPT, as well as its background, current state of technology, advantages, disadvantages, and uses. This allows us to understand the increased potential for long-term, straightforward transfer of electricity with minimal losses. It is anticipated that wireless energy could be achieved with the benefit of being simple to set up and less costly, meaning that the research of transmission and distribution overhead would decrease. Additionally, it is very important to know that the research of electrical power on the consumer would even decrease in comparison to current systems. A revolutionary converter architecture that is appropriate for EV dynamic charging is being introduced as a whole. There are benefits to the suggested architecture over current ones, including less complexity and switching device requirements. A mathematical framework has been created to explain the boundary circumstances for the primary modes of operation and to forecast the system's total power transfer. The correctness of the suggested mathematical framework and the innovative architecture are confirmed by the outcomes of an actual prototype system and a numerical calculation.

References

1) P. K.-H. Dost, P. Spichartz and C. Sourkounis, "Charging Behavior of Users Utilizing Battery Electric Vehicles and Extended Range Electric Vehicles Within the Scope of a Field Test," in IEEE Transactions on Industry Applications, vol. 54, no. 1, pp. 580-590, Jan.-Feb. 2018.

2) E. ElGhanam, H. Sharf, Y. Odeh, M. S. Hassan and A. H. Osman, "On the Coordination of

Power System Technology
ISSN:1000-3673
Received: 16-01-2024 Revised: 12-02-2024 Accepted: 07-03-2024

Charging Demand of Electric Vehicles in a Network of Dynamic Wireless Charging Systems," in IEEE Access, vol. 10, pp. 62879-62892, 2022.
3) A. Rezaei, J. B. Burl, M. Rezaei and B. Zhou, "Catch Energy Saving Opportunity in Charge-Depletion Mode, a Real-Time Controller for Plug-In Hybrid Electric Vehicles," in IEEE Transactions on Vehicular Technology, vol. 67, no. 11, pp. 11234-11237, Nov. 2018.
Applied
4) H.-S. Gu and H.-S. Choi, "Analysis of Wireless Power Transmission Characteristics for High-Efficiency Resonant Coils," in IEEE Transactions on Superconductivity, vol. 30, no. 4, pp. 1-4, June 2020, Art no. 5400304.
5) Y. Bu, S. Endo and T. Mizuno, "Improvement in the Transmission Efficiency of EV Wireless Power Transfer System Using a Magnetoplated Aluminum Pipe," in IEEE Transactions on Magnetics, vol. 54, no. 11, pp. 1-5, Nov. 2018.
6) S. Li, L. Wang, Y. Guo, C. Tao and L. Ji, "Power Stabilization With Double Transmitting Coils and T-Type Compensation Network for Dynamic Wireless Charging of EV," in IEEE Journal of Emerging and Selected Topics in Power Electronics, vol. 8, no. 2, pp. 1801-1812, June 2020.
7) L. Wang, U. K. Madawala and M. -C. Wong, "A Wireless Vehicle-to-Grid-to-Home Power Interface With an Adaptive DC Link," in IEEE Journal of Emerging and Selected Topics in Power Electronics, vol. 9, no. 2, pp. 2373-2383, April 2021.
8) M. Rozman et al., "Smart Wireless Power Transmission System for Autonomous EV Charging," in IEEE Access, vol. 7, pp. 112240-112248, 2019.
9) P. K. Joseph, D. Elangovan and P. Sanjeevikumar, "System Architecture, Design, and Optimization of a Flexible Wireless Charger for Renewable Energy-Powered Electric Bicycles," in IEEE Systems Journal, vol. 15, no. 2, pp. 2696-2707, June 2021.
10) D. Vincent, P. S. Huynh, N. A. Azeez, L. Patnaik and S. S. Williamson, "Evolution of Hybrid Inductive and Capacitive AC Links for Wireless EV Charging A Comparative Overview," in IEEE Transactions on Transportation Electrification, vol. 5, no. 4, pp. 1060-1077, Dec. 2019.
11) Y. Zhang, W. Zhang, F. Gao, S. Gao and D. J. Rogers, "A Switched-Capacitor Interleaved Bidirectional Converter With Wide Voltage-Gain Range for Super Capacitors in EVs," in IEEE Transactions on Power Electronics, vol. 35, no. 2, pp. 1536-1547, Feb. 2020.
12) Y. Zhang, X. -F. Cheng, C. Yin and S. Cheng, "A Soft-Switching Bidirectional DC- DC Converter for the Battery Super-Capacitor Hybrid Energy Storage System," in IEEE Transactions on Industrial Electronics, vol. 65, no. 10, pp. 7856-7865, Oct. 2018. 13) M. Safayatullah, M. T. Elrais, S. Ghosh, R. Rezaii and I. Batarseh, "A Comprehensive Review of Power Converter Topologies and Control Methods for Electric Vehicle Fast

Power System Technology
ISSN:1000-3673
Received: 16-01-2024 Revised: 12-02-2024 Accepted: 07-03-2024

Charging Applications," in IEEE Access, vol. 10, pp. 40753-40793, 2022.

14) J. Wu, S. Li, S.-C. Tan and S. Y. R. Hui, "Capacitor-Clamped LLC Resonant Converter Operating in Capacitive Region for High-Power-Density EV Charger," in IEEE Transactions on Power Electronics, vol. 36, no. 10, pp. 11456-11468, Oct. 2021. 15) S.-K. Lim, H.-S. Lee, H.-R. Cha and S. -J. Park, "Multi-Level DC/DC Converter for E-Mobility Charging Stations," in IEEE Access, vol. 8, pp. 48774-48783, 2020. 16) N. D. Dao, D.-C. Lee and Q. D. Phan, "High-Efficiency SiC-Based Isolated Three-Port DC/DC Converters for Hybrid Charging Stations," in IEEE Transactions on Power Electronics, vol. 35, no. 10, pp. 10455-10465, Oct. 2020.

17) Y. Xuan, X. Yang, W. Chen, T. Liu and X. Hao, "A Novel Three-Level CLLC Resonant DC-DC Converter for Bidirectional EV Charger in DC Microgrids," in IEEE Transactions on Industrial Electronics, vol. 68, no. 3, pp. 2334-2344, March 2021. 18) R. Kushwaha and B. Singh, "Design and Development of Modified BL Luo Converter for PQ Improvement in EV Charger," in IEEE Transactions on Industry Applications, vol. 56, no. 4, pp. 3976-3984, July-Aug. 2020. 19) H. Heydari-doostabad and T. O'Donnell, "A Wide-Range High-Voltage-Gain Bidirectional DC-DC Converter for V2G and G2V Hybrid EV Charger," in IEEE Transactions on Industrial Electronics, vol. 69, no. 5, pp. 4718-4729, May 2022. 20) S. Jia, C. Chen, S. Duan and Z. Chao, "Dual-Side Asymmetrical Voltage-Cancelation Control for Bidirectional Inductive Power Transfer Systems," in IEEE Transactions on Industrial Electronics, vol. 68, no. 9, pp. 8061-8071, Sept. 2021.

21) K. Inoue, K. Kusaka and J. -I. Itoh, "Reduction in Radiation Noise Level for Inductive Power Transfer Systems Using Spread Spectrum Techniques," in IEEE Transactions on Power Electronics, vol. 33, no. 4, pp. 3076-3085, April 2018.

22) V. M. Iyer, S. Gulur, G. Gohil and S. Bhattacharya, "An Approach Towards Extreme Fast Charging Station Power Delivery for Electric Vehicles with Partial Power Processing," in IEEE Transactions on Industrial Electronics, vol. 67, no. 10, pp. 8076- 8087, Oct. 2020.

23) M. -Z. Lu, Z.-W. Guo and C. -M. Liaw, "A Battery/Supercapacitor Hybrid Powered EV SRM Drive and Microgrid Incorporated Operations," in IEEE Transactions on Transportation Electrification, vol. 7, no. 4, pp. 2848-2863, Dec. 2021.

24) Z. Wang, Y. Zhang, S. You, H. Xiao and M. Cheng, "An Integrated Power Conversion System for Electric Traction and V2G Operation in Electric Vehicles With a Small Film Capacitor," in IEEE Transactions on Power Electronics, vol. 35, no. 5, pp. 5066-5077, May 2020.

25) Z. Gao and Q. Lu, "A Hybrid Cascaded Multilevel Converter Based on Three-Level Cells for Battery Energy Management Applied in Electric Vehicles," in IEEE Transactions on Power Electronics, vol. 34, no. 8, pp. 7326-7349, Aug. 2019.

Power System Technology
ISSN:1000-3673

Received: 16-01-2024 *Revised: 12-02-2024* *Accepted: 07-03-2024*

26) K. Subramanian and S. Kumarasamy, “Performance Identification Using Morphological Approach on Digital Mammographic Images,” Curr. Signal Transduct. Ther., vol. 11, no. 2, 2016, doi: 10.2174/1574362411666160617102315.
27) P. Sreelatha, M. S. Udayakumar, S. Karthick, S. C. Ch, K. C. S. Kavya, and M. Madiajagan, “Managing The Tomato Leaf Disease Detection Accuracy Using Computer Vision Based Deep Neural Network,” J. Contemp. Issues Bus. Gov. Vol, vol. 27, no. 1, pp. 3425–3437, 2021.
28) P. Saranya, S. Karthick, and C. Thulasiyammal, “Image processing method to measure the severity of fungi,” Int. J. Adv. Res., vol. 2, no. 2, pp. 95–100, 2014, [Online]. Available: https://www.journalijar.com/article/775/image-processing-method-to-measure-the-severity-of-fungi-caused-disease-in-leaf